Supplementary Information

A multi-functional nano-platform based on $LiGa_{4.99}O_8:Cr_{0.01}/IrO_2$ with near infrared–persistent luminescence, "afterglow" photodynamic and photo–thermal functions

Xiangyu Liu [a], Rujie Xi [a], Yanfang Hu [a], Yong Wang [b] and Abdukader Abdukayum [a,*]

[a] Xinjiang Key Laboratory of Novel Functional Materials Chemistry，College of Chemistry and Environmental Sciences, Kashi University, Kashi 844000, China

[b] State Key Laboratory of Radiation Medicine and Protection, School for Radiological and Interdisciplinary Sciences (RAD-X), Collaborative Innovation Center of Radiation Medicine of Jiangsu Higher Education Institutions, Soochow University, Suzhou 215123, China

Corresponding authors:

Prof. Dr. A. Abdukayum (E-mail: abdukadera@sina.com);

Table of Contents

1.Material and Methods

1.1 Material

$LiNO_3$ (99.99%), Ga_2O_3 (99.99%), $Cr(NO_3)_3 \cdot 9H_2O$ (99.99%), (3-aminopropyl)triethoxysilane (APTES) (98%), 3-chloropropyltrimethoxysilane (CPTMS) (98%), N-hydroxybutanediimide (NHS) (95%), N,N-dimethylformamide (DMF) (A.R) were purchased from Shanghai Aladdin Biochemical Technology Co. $IrCl_3$ (99.99%) was purchased from Alfa Aesar Chemicals Ltd. 1-(3-dimethylaminopropyl)-3-ethylcarbodiimide hydrochloride (EDC-HCl) (99%), 1,3-diphenylisobenzofuran (DPBF) (97%) were purchased from Shanghai Macklin Biochemistry Technology Co. Polyethylene glycol (MW=2000) was purchased from Beijing Royaltech Technology Co. K_2CO_3 (99%), ethylene glycol ($C_2H_6O_2$) (99.21%) were purchased from Shanghai Bide Pharmatech Ltd. $NH_3 \cdot H_2O$ (A.R), anhydrous ethanol (A.R) were purchased from Tianjin Xinbute Chemical Co. Toluene (C_7H_8) (99.5%), HCl (A.R), HNO_3 (A.R), NaOH (97%) were purchased from Chengdu Cologne Chemical Co.

1.2 Characterizations

The chemical composition and crystal structure of the samples were

analyzed by using an X-ray diffraction spectrometer (XRD) of type D8 ADVANCE with working source CuKα from Bruker, Germany. The morphology and particle size of the samples were observed by using a JEM-2100F transmission electron microscope (TEM) from JEOL, Japan. Photoluminescence spectra were recorded on an FS5C spectrofluorometer (Edinburgh Instruments, UK). The afterglow decay curves were obtained using a FS5C fluorescence spectrometer and the samples were excited with a 254 nm UV lamp for 5 min before the test. The afterglow decay images of LGO:Cr and LGO:Cr/IrO_2 were taken using a Roper Lumazone series LUMO plant and animal fluorescence in vivo imaging system and samples were excited with a 254 nm UV lamp for 10 min before testing began. The fourier transform infrared spectroscopy (FT-IR) spectra were obtained from Thermo IR-200, Thermo Fisher Scientific, USA. The UV-Vis absorption spectra were tested by UV-2600 of SHIMADZU, Japan. The hydrodynamic size and zeta potential of materials were obtained by BeNano 180 Zeta Pro (Dandong bettersize Instruments Co). X-ray photoelectron spectroscopy were obtained from the ESCALAB 250Xi of Thermo Fisher Scientific, USA. The thermoluminescence spectra were obtained from TOSL-3DS of Guangzhou Rongfan Technology Co. It was excited by a 254 nm UV lamp for 10 min before the test, with a test wavelength range of 300-850 nm. The temperature measurement range of 298-773 K and temperature increase rate of 5 K/s. The infrared diode

laser model is MDL-XF-808-10W and the photo-thermal photographs were obtained from a FLIR E75 infrared camera from the USA. The quantum yield was tested by F-7100 of HITACHI, Japan. The electron spin resonance (ESR) spectra were obtained from paramagnetic resonance spectrometer (Bruker A300, Germany).

1.3 Synthesis of $LiGa_{5-x}O_8:Cr_x$

In this paper, $LiGa_{5-x}O_8:Cr_x$ (x=0.002, 0.004, 0.006, 0.008, 0.01, 0.012) PLNPs were prepared by glycol-assisted hydrothermal synthesis. Firstly, Li^+ (0.2 M), Ga^{3+} (0.2 M) (Ga_2O_3 dissolved in concentrated nitric acid) and Cr^{3+} (0.01 M) were dissolved in ethylene glycol and stirred. Next, the pH of the solution was adjusted to 11 and stirring was resumed. Subsequently, the above solution was transferred to an autoclave and reacted for 24 h at 443 K. The above PLNPs were washed with anhydrous ethanol and ultrapure water, and then dried it. Finally, it calcined at 973 K for 3 h.

1.4 Synthesis of IrO_2 NPs

The method of preparation in this paper is based on previous literature methods and improved. Firstly, $IrCl_3$ was added to 50 mL of ultrapure water and the solution was stirred for 3 h. Afterwards, it was

allowed to stand at 277 K for about 3 d until the solution became clear. Secondly, the above solution was allowed to stand at room temperature for about 2 h. Subsequently, NaOH solution (1.0 M) was added drop by drop to adjust the pH to 12 and the mixture was further stirred at room temperature for about 2.5 h. Finally, the mixture was then allowed to react at 353 K with vigorous stirring under condensation for 10 min. The final product was washed three times with anhydrous ethanol, dialyzed and lyophilized.

1.5 Construction of a multifunctional nanoplatform of LGO:Cr/IrO_2

Firstly, the synthesized LGO:Cr was dispersed into 5 mM NaOH solution (100 mL) and sonicated for 10 min, and then stirred vigorously at room temperature for 24 h. Secondly, LGO-OH (100 mg) was dispersed in DMF (50 mL) and CPTMS (200 μL) was added drop by drop, and then refluxed for 24 h at 353 K. Thirdly, the final product was washed with DMF and anhydrous ethanol twice each, and then dried to obtain LGO-Si-Cl.

The dried IrO_2 NPs (70 mg) powder was dispersed in DMF (30 mL) by sonication and APTES (280 μL) was added drop by drop, and then stirred in an oil bath at 353 K for 24 h. The above mixture was washed with DMF for three times to remove unreacted APTES, dialyzed and

lyophilized to obtain IrO_2-NH_2. Weighed the powder of mPEG-COOH (0.2 mmol), added EDC (0.4 mmol), NHS (1.0 mmol), and dispersed in 15 mL of DMF by sonication for 30 min, and then reacted for 12 h in the dark. Then, put into IrO_2-NH_2 (45 mg) to continue the reaction for 3 d. After the reaction was finished, dialysis and lyophilization were carried out, and the IrO_2-PEG was obtained.

LGO-Si-Cl (5 mmol), IrO_2-PEG (5 mmol) and K_2CO_3 (5 mmol) were added in toluene (60 mL) solution, and then refluxed at 388 K for 12 h. After the reaction was finished, dialysis and lyophilization were carried out, and the final products of LGO:Cr/IrO_2 were obtained.

1.6 Photodynamic experiment

The IrO_2 group and the LGO:Cr/IrO_2 group were mixed with TEMP solution, irradiated by 254 nm for 2 min, and immediately detected by ES R spectroscopy for $^1O_2$ production. DPBF can be evaluated for ROS generation by UV-Vis absorption spectrum. 20 μL of DPBF solution (10 mM ethanol solvent) was added to 1980 μL of IrO_2 (100 μg/mL) and LGO:Cr/IrO_2 (100 μg/mL, 200 μg/mL, 400 μg/mL, 800 μg/mL, 1000 μg/mL) aqueous ethanol solutions (CH_3CH_2OH:H_2O=4:6) , respectively. Subsequently, the mixture was irradiated with 254 nm lamp and the absorbance of DPBF at 413 nm was recorded every 2 min.

1.7 Photo-thermal experiment

In order to evaluate the PTT effect of LGO:Cr/IrO_2. Firstly, 1.0 mL of H_2O, IrO_2 NPs and LGO:Cr/IrO_2 solution were taken and added to 1.5 mL PE tubes, respectively. Then, irradiated with 808 nm laser (3.9 W·cm^{-2}) for 600 s and the temperature changes were recorded by infrared thermal imager every 30 s. Next, 1.0 mL of LGO:Cr/IrO_2 solution was added to a 1.5 mL PE tube and irradiated with an 808 nm laser for 600 s. The temperature changes of the solution were determined at different laser power densities (1.3, 2.6, 3.9, 5.2 and 6.5 W·cm^{-2}). Finally, 1.0 mL of LGO:Cr/IrO_2 solution with concentrations of 0 μg/mL, 50 μg/mL, 100 μg/mL, 200 μg/mL, 400 μg/mL, 800 μg/mL, and 1000 μg/mL, respectively. The above solution was added to a 1.5 mL PE tube and irradiated with an 808 nm laser (3.9 W·cm^{-2}) for 600 s, and then the temperature changes were recorded by an infrared thermal imager every 30 s. In addition, 1.0 mL of 1000 μg/mL LGO:Cr/IrO_2 solution was taken in a 1.5 mL PE tube, irradiated with 808 nm (3.9 W·cm^{-2}) laser for 5 min. Afterwards, the laser was turned off for 10 min and the temperature change of the process was recorded with an infrared thermal imager every 30 s. The process was cycled for 5 times, which was used to evaluate the PTT stability of LGO:Cr/IrO_2.

1.8 Measurement of the percentages of the ionic radii of Li^+ and

$Ga1^{3+}$ in relation to Cr^{3+}.

$$D_r = [|R_m(CN) - R_d(CN)|]/R_m(CN) \quad (1)$$

The R_m is the ionic radius of Li^+ and $Ga1^{3+}$, and R_d is the ionic radius of Cr^{3+}.

1.9 Measurement of the average depth of the electron-trap energy level.

$$E = \frac{2KT_m^2}{T_h - T_m} \quad (2)$$

The E is the average electron-trap energy level (eV), K is Boltzmann's constant (eV), T_m is the peak temperature (K), and T_h is the half-peak temperature (K).

1.10 Measurement of the persistent luminous efficiency.

$$\Phi = \Phi_d - (1 - A_d)\,\Phi_i \quad (3)$$

The φ_d is the direct excitation quantum yield, φ_i is the indirect excitation quantum yield, and A_d is the direct excitation absorption rate.

1.11 Measurement of the energy transfer efficiency.

$$E = \frac{F_D - F_{DA}}{F_D} \quad (4)$$

The F_D and F_{DA} are the fluorescence intensity of the donor (LGO:Cr) alone and the donor in the presence of acceptor (LGO:Cr/IrO_2), respectively.

1.12 Measurement of photo-thermal conversion efficiency.

$$\eta = \frac{hS(T_{max,NPs} - T_{max,solvent})}{I(1-10^{-A808})} \quad (5)$$

$$\tau_s = \frac{m_D C_D}{hS} \quad (6)$$

$$t = -\tau_s \ln \theta \quad (7)$$

$$\theta = \frac{T - T_{surr}}{T_{max,NPs} - T_{surr}} \quad (8)$$

The h is the heat transfer coefficient, S is the surface area of the container, $T_{max,NPs}$ and $T_{max,solvent}$ are maximum steady-state temperature for NPs solution and water, which are 50.0 and 33.0 °C, respectively. I is the incident laser power (3.9 $W \cdot cm^{-2}$), and A_{808} is the absorbance of the NPs at 808 nm (A_{808}=0.36). τs is the sample system time constant, and m_D and C_D are the mass (1.0 g) and heat capacity (4.2 $J \cdot g^{-1}$) of the

deionized water used as the solvent, respectively. θ is the dimensionless driving force temperature, T_{surr} is the ambient temperature of the surroundings, T is a temperature for NPs solutions at a constant cooling time (t), and τ_s can be determined by applying the linear time data from the t vs −ln θ (τ_s=194.6 s) .

2. Table

Table S1. The parameters of photoluminescence decay curve fitting.

$$I_{(t)} = I_{(0)} + A_1 \exp\left(\frac{t}{\tau_1}\right) + A_2 \exp\left(\frac{t}{\tau_2}\right) + A_3 \exp\left(\frac{t}{\tau_3}\right) \quad (9)$$

$$\tau_{av} = \frac{A_1\tau_1^2+A_2\tau_2^2+A_3\tau_3^2}{A_1\tau_1+A_2\tau_2+A_3\tau_3} \quad (10)$$

Sample	τ_1	A_1	τ_2	A_2	τ_3	A_3	τ_{av}
LGO:Cr	30.89	110072	3.017	106248	172.6	40864	122.8
LGO:Cr/IrO_2	4.54	13658	19.33	11734	104.9	2952	94

3. Figures

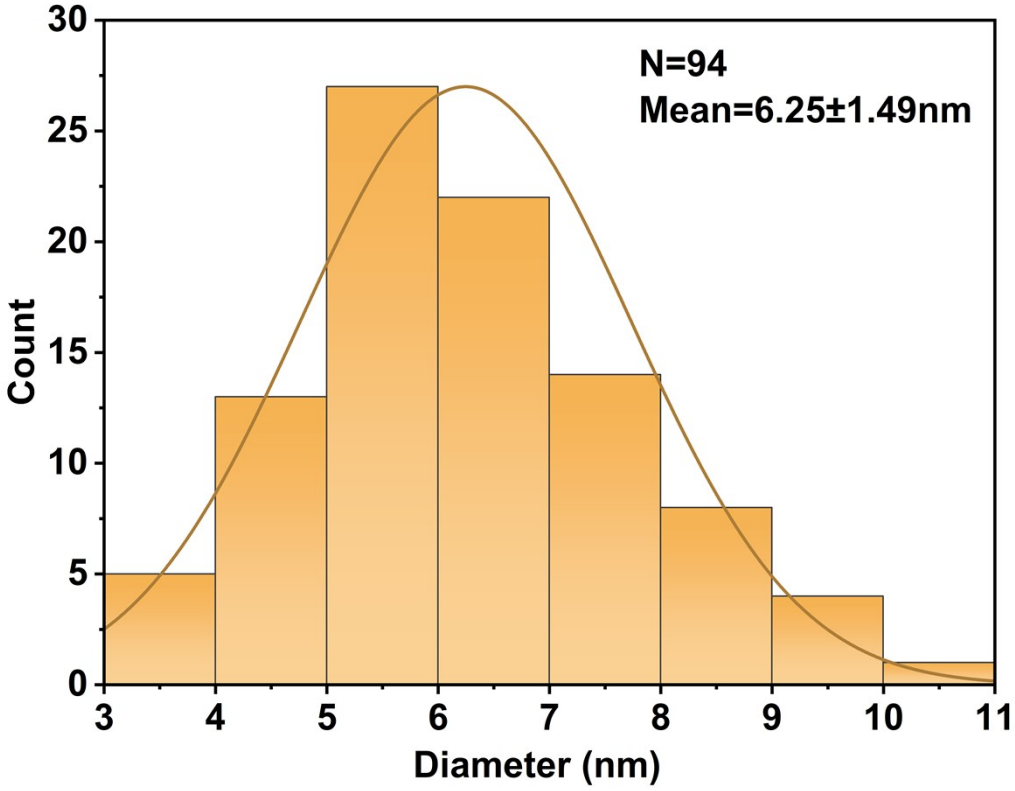

Figure S1. Particle size statistical chart of LGO:Cr.

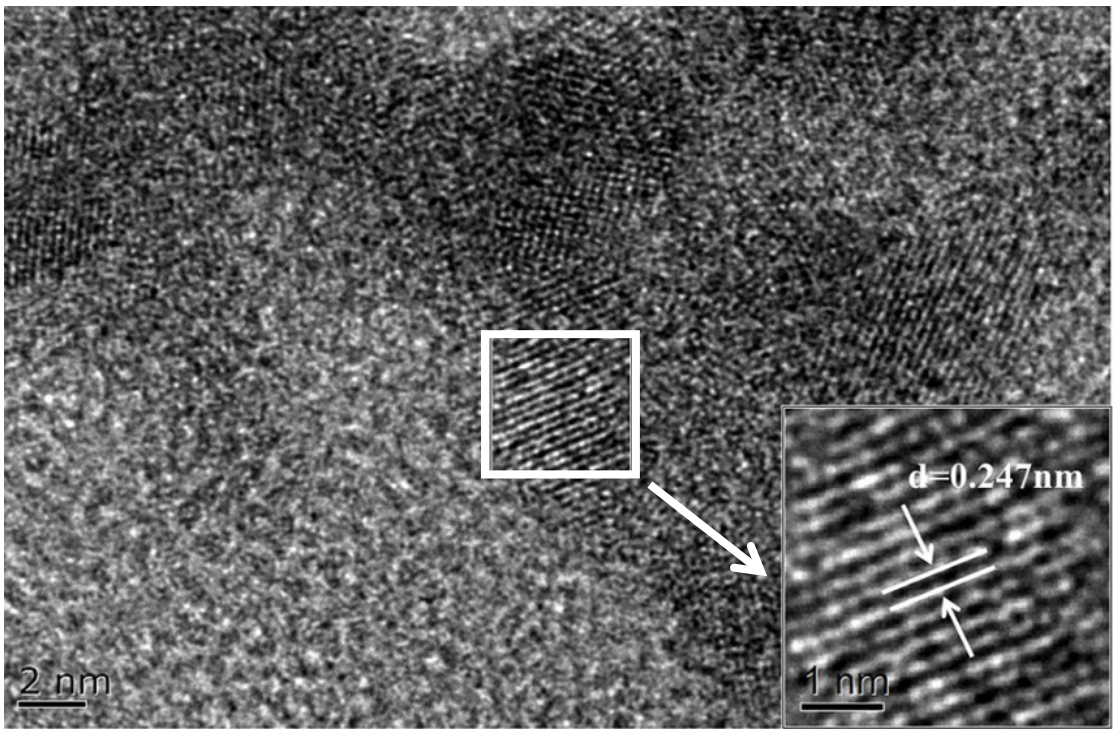

Figure S2. HRTEM image of LGO:Cr.

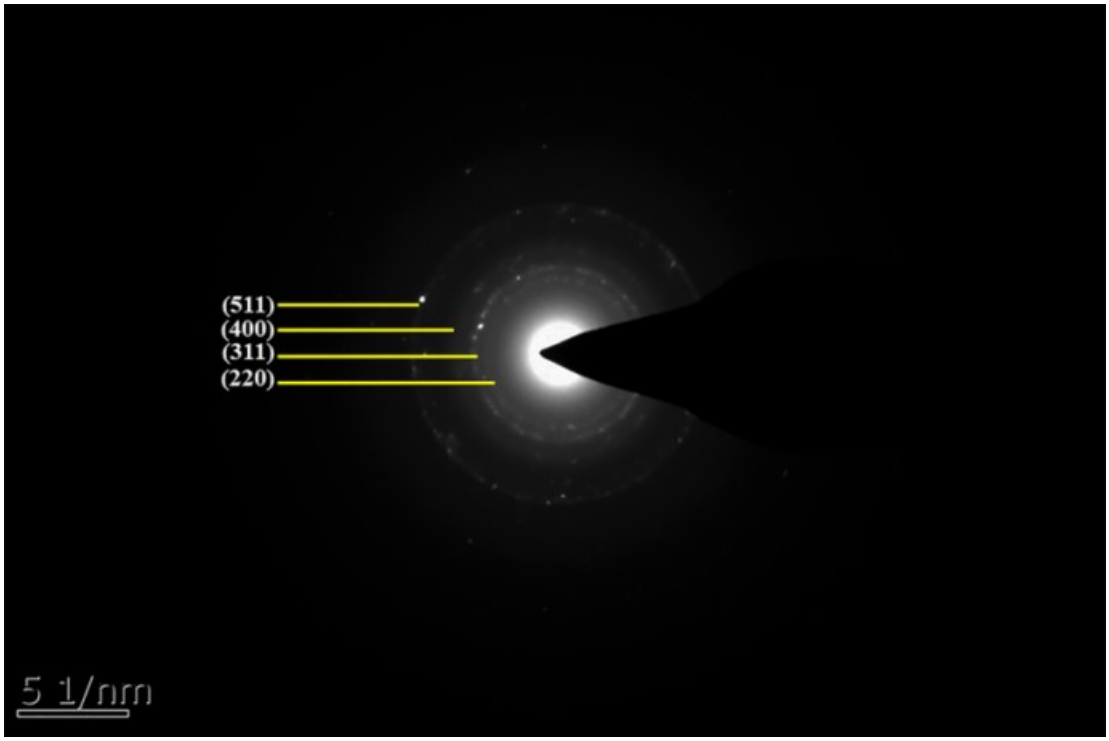

Figure S3. SADE image of LGO:Cr.

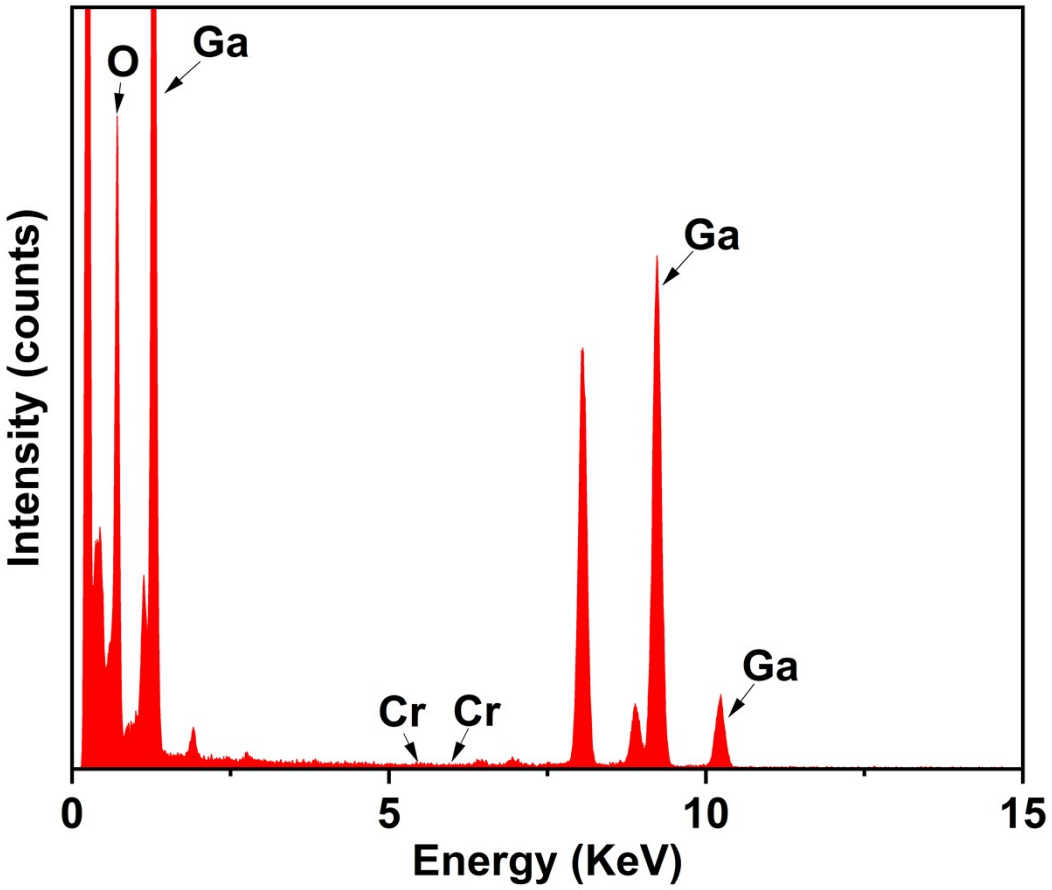

Figure S4. EDS analysis of LGO:Cr.

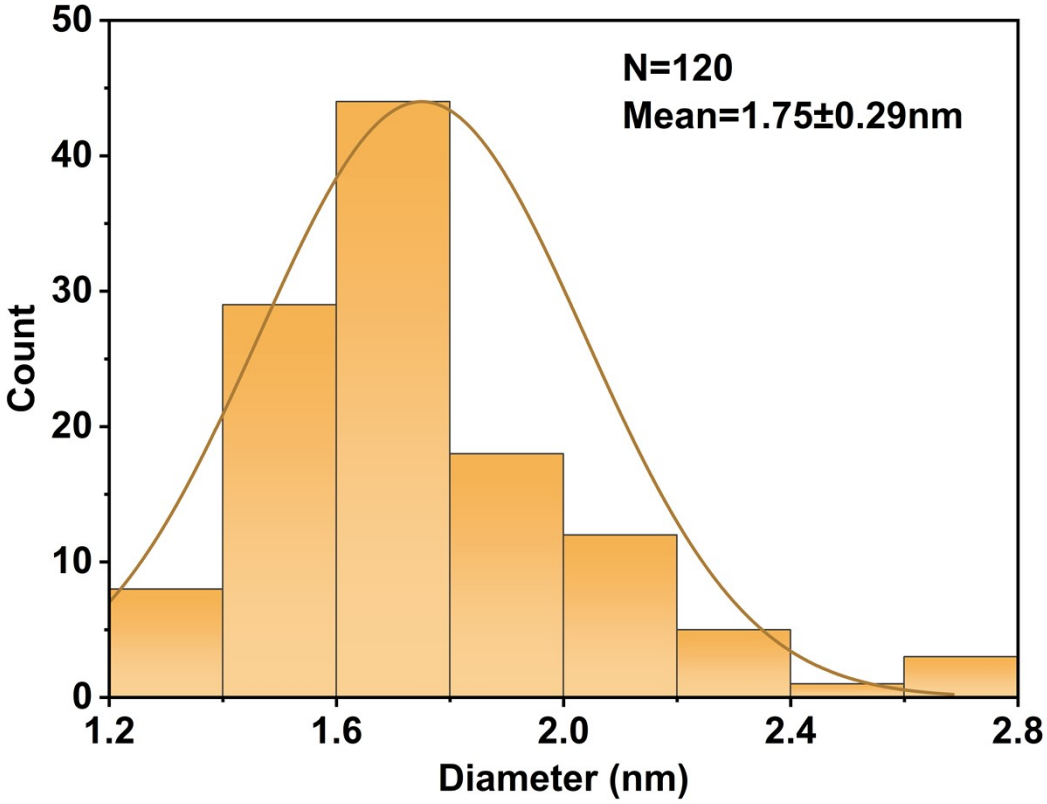

Figure S5. Particle size statistical chart of IrO_2 NPs.

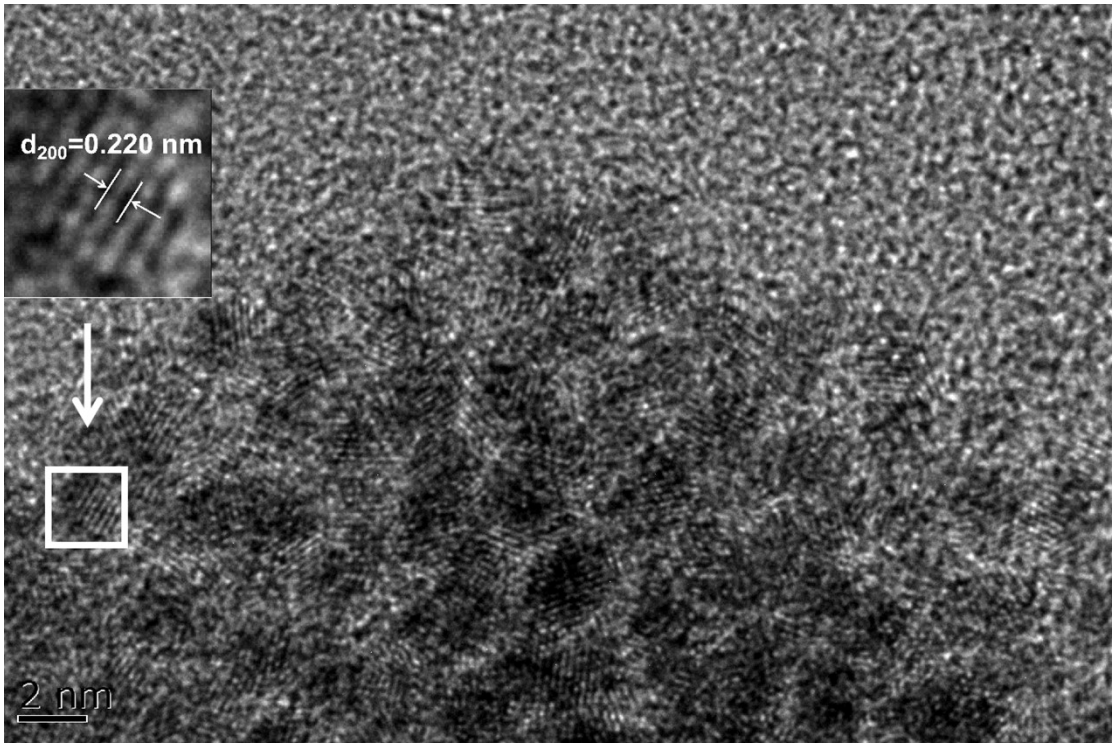

Figure S6. HRTEM image of IrO_2 NPs.

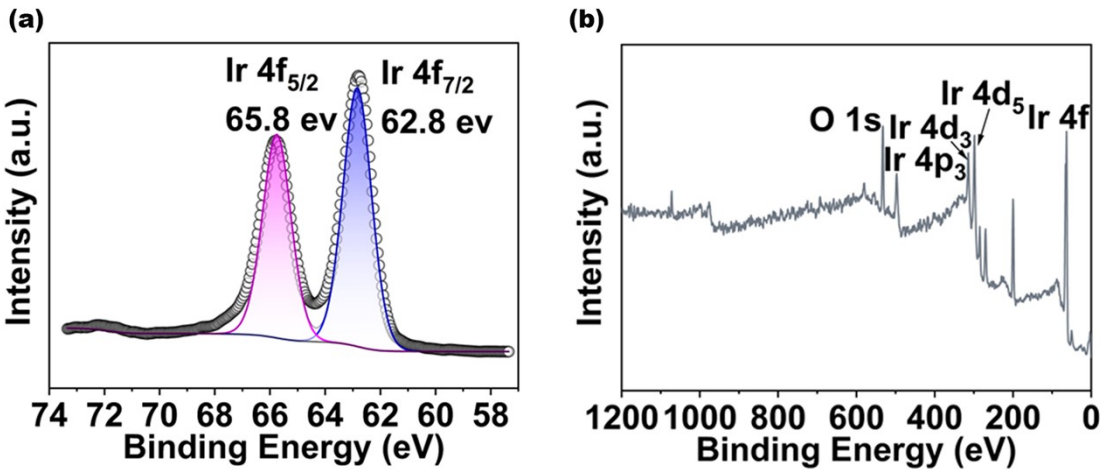

Figure S7. (a-b) XPS analysis of IrO_2 NPs.

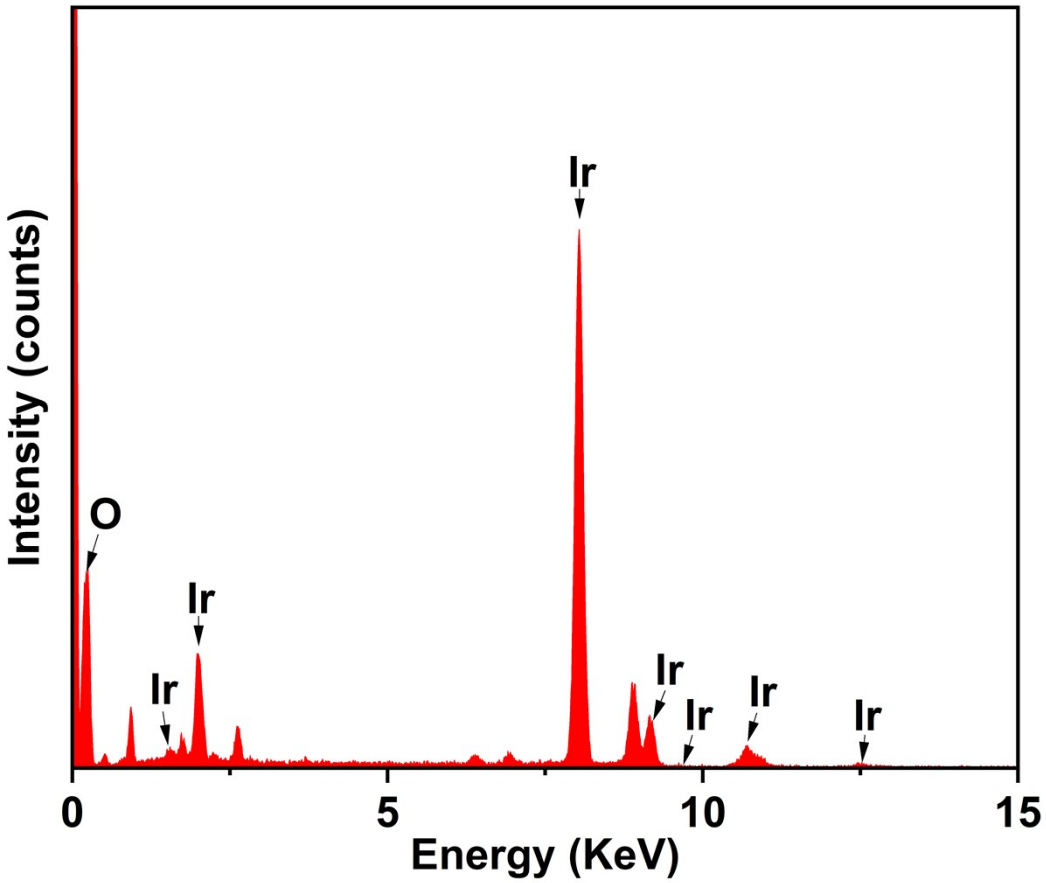

Figure S8. EDS analysis of IrO_2 NPs.

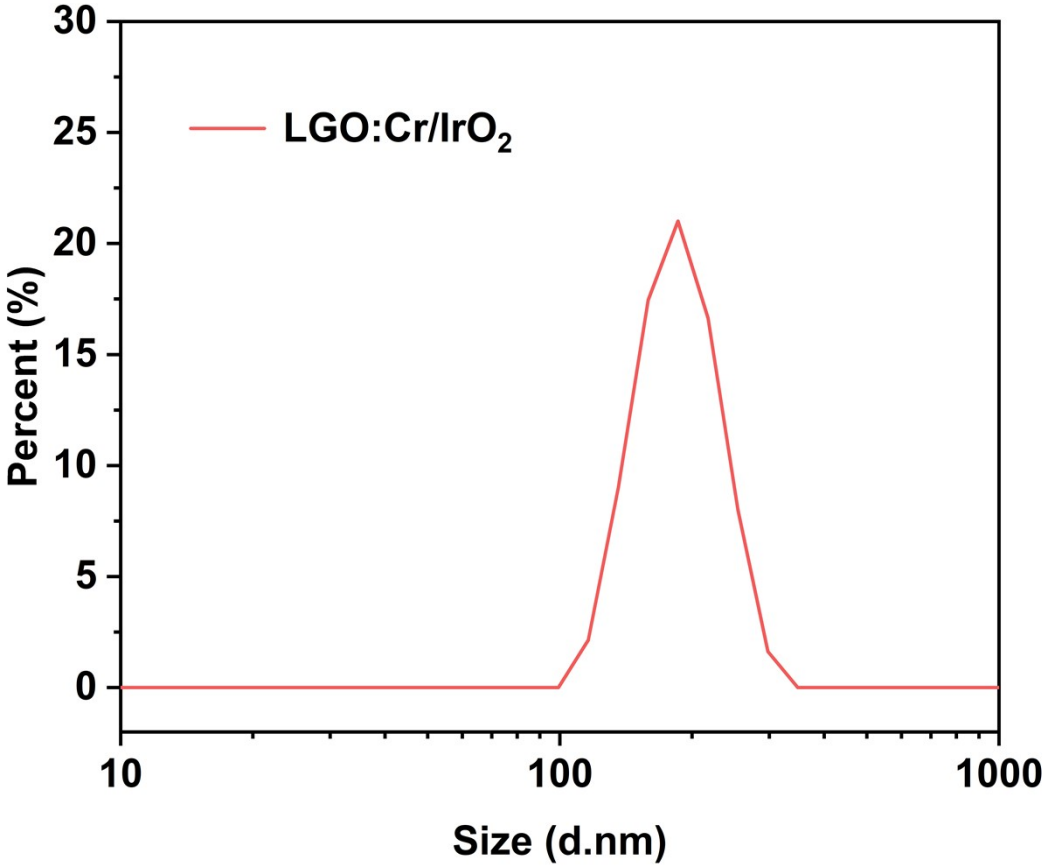

Figure S9. DLS analysis of LGO:Cr/IrO_2.

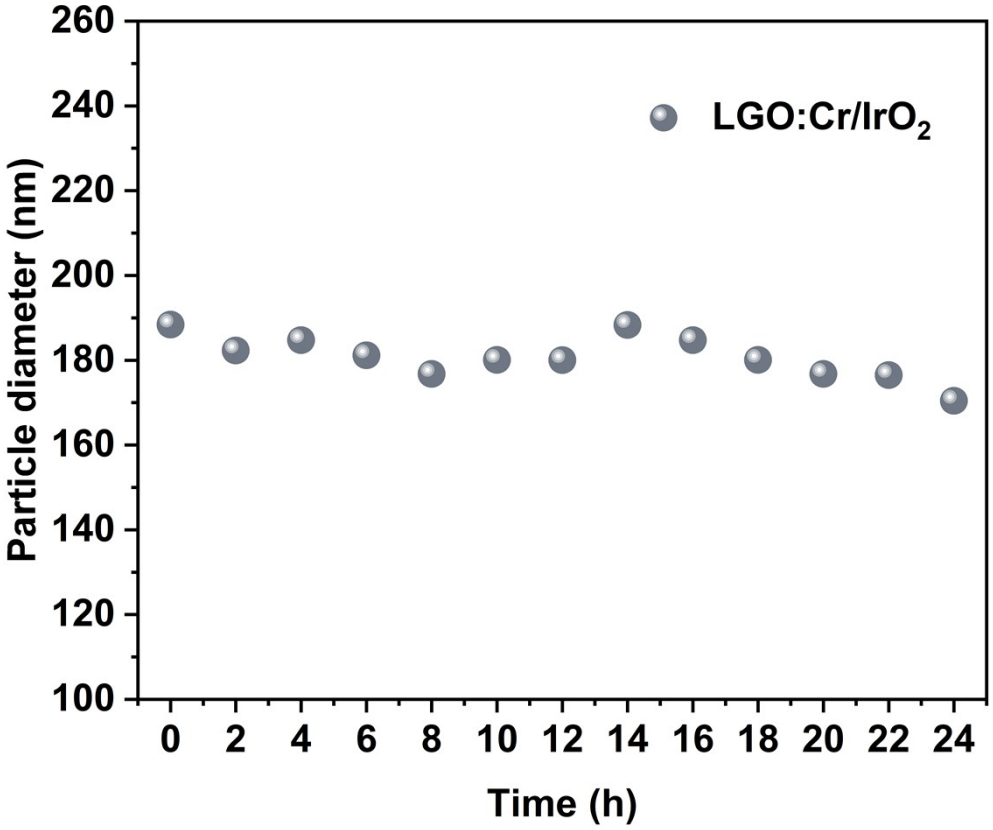

Figure S10. The stability of LGO:Cr/IrO_2.

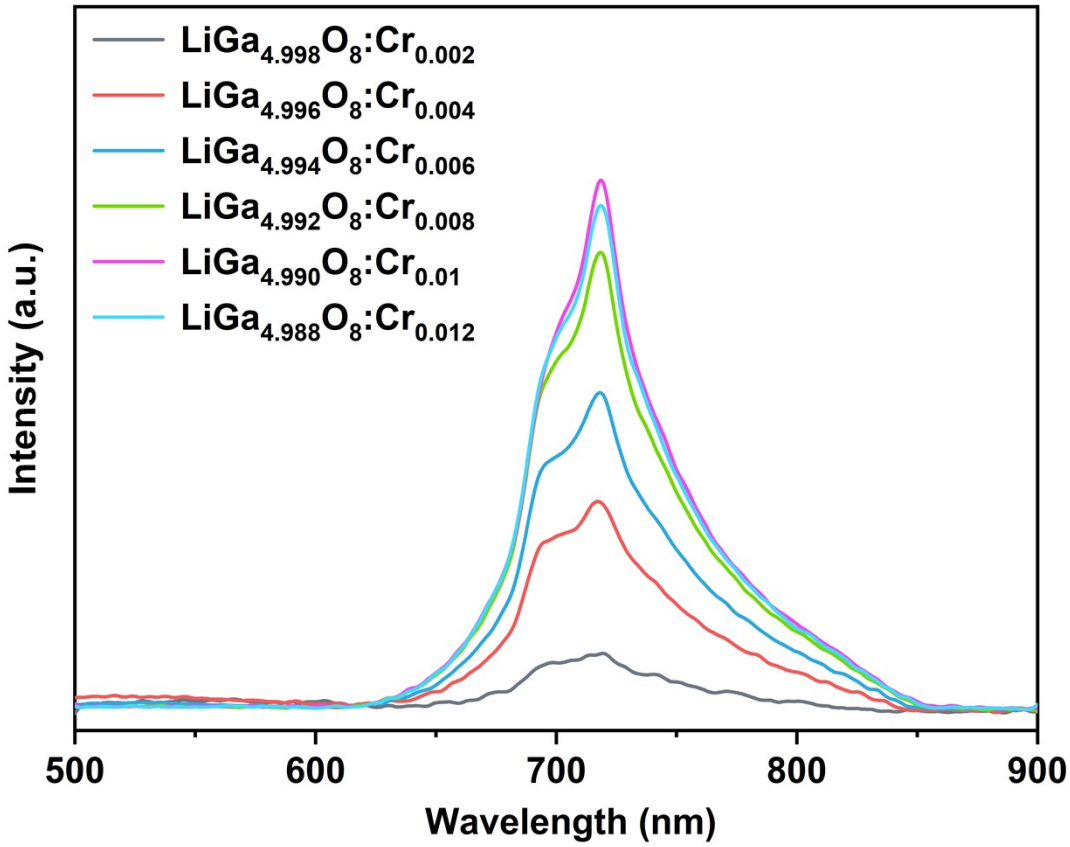

Figure S11. Photoluminescence spectra of $LiGa_{5-x}O_8:Cr_x$ (x=0.002, 0.004, 0.006, 0.008, 0.01, 0.012) at the excitation wavelength of 254 nm.

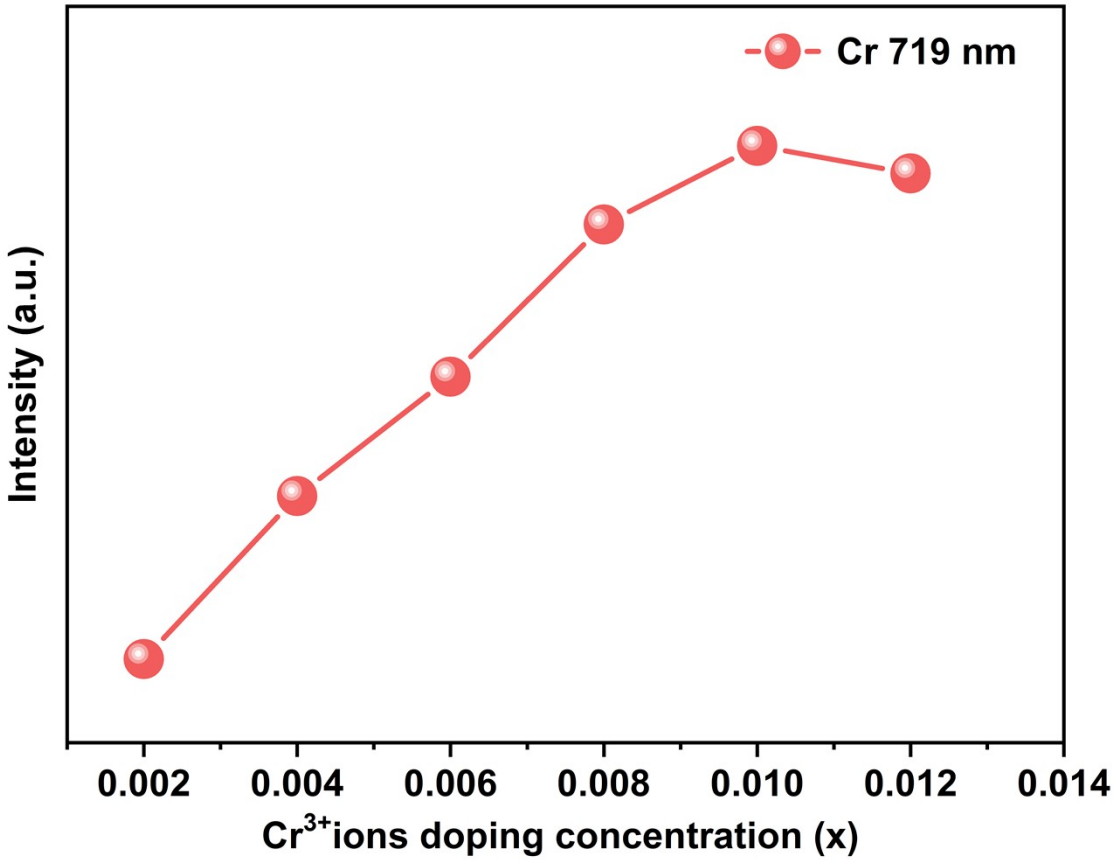

Figure S12. The reIationship between the Photoluminescence spectra intensity of $LiGa_{5-x}O_8:Cr_x$ and doping concentrations of Cr^{3+} ions.

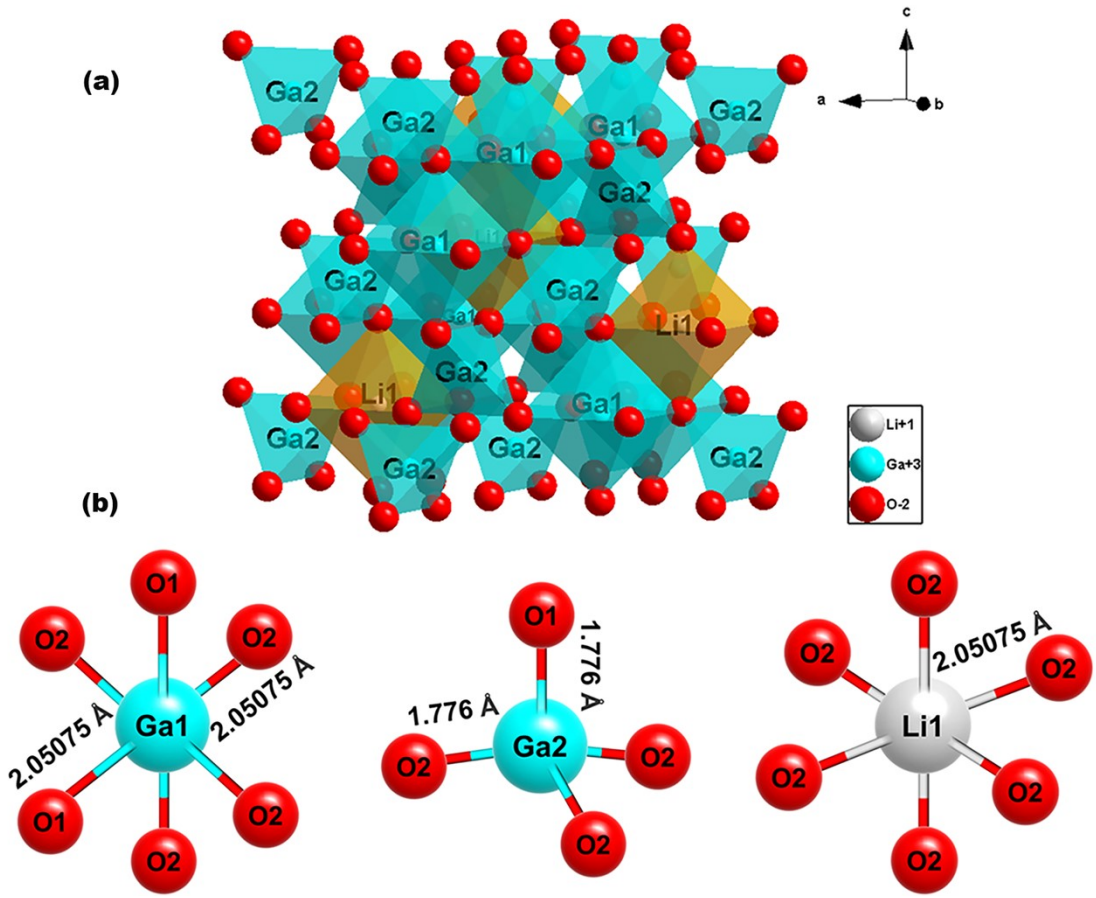

Figure S13. (a-b) The crystal structure of $LiGa_5O_8$ which was redrawn on the basis of PDF 38-1171 using Diamond program.

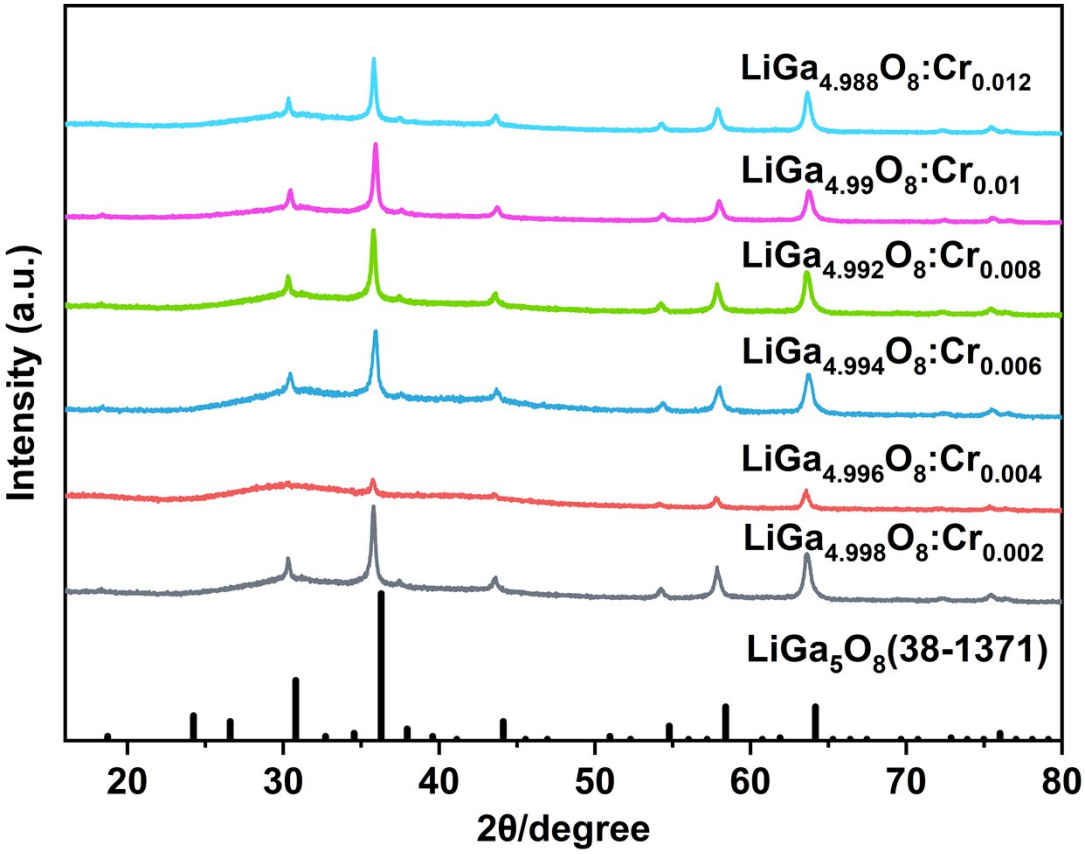

Figure S14. XRD pattern of $LiGa_{5-x}O_8:Cr_x$ (x=0.002, 0.004, 0.006, 0.008, 0.01, 0.012).

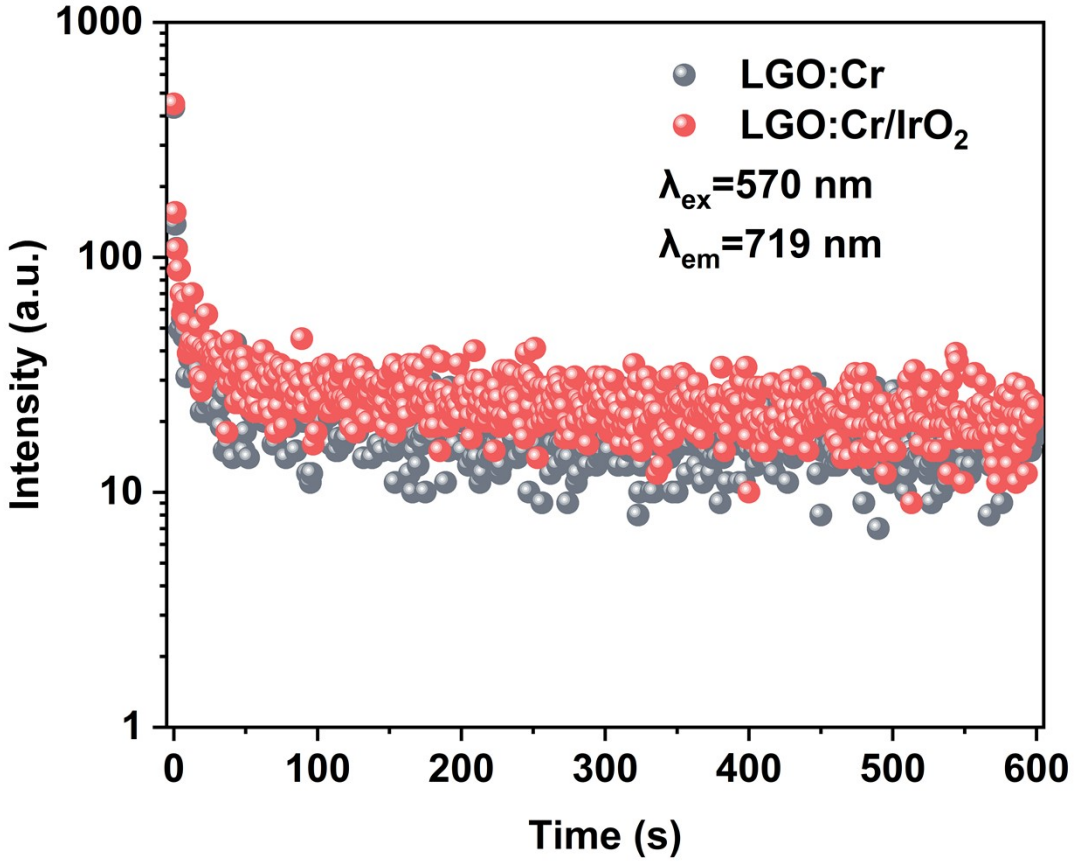

Figure S15. Afterglow decay curves of LGO:Cr and LGO:Cr/IrO_2 after 5 min of 570 nm visible light irradiation.

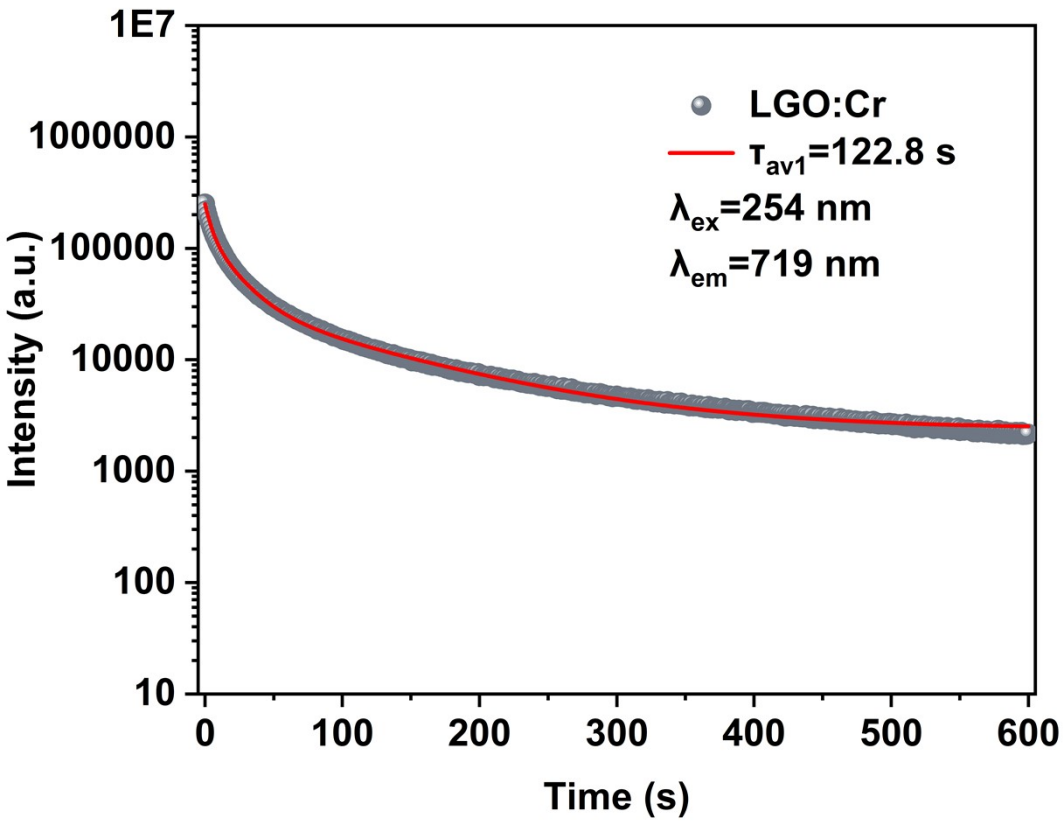

Figure S16. Afterglow decay curves of LGO:Cr after 5 min of 254 nm UV light irradiation.

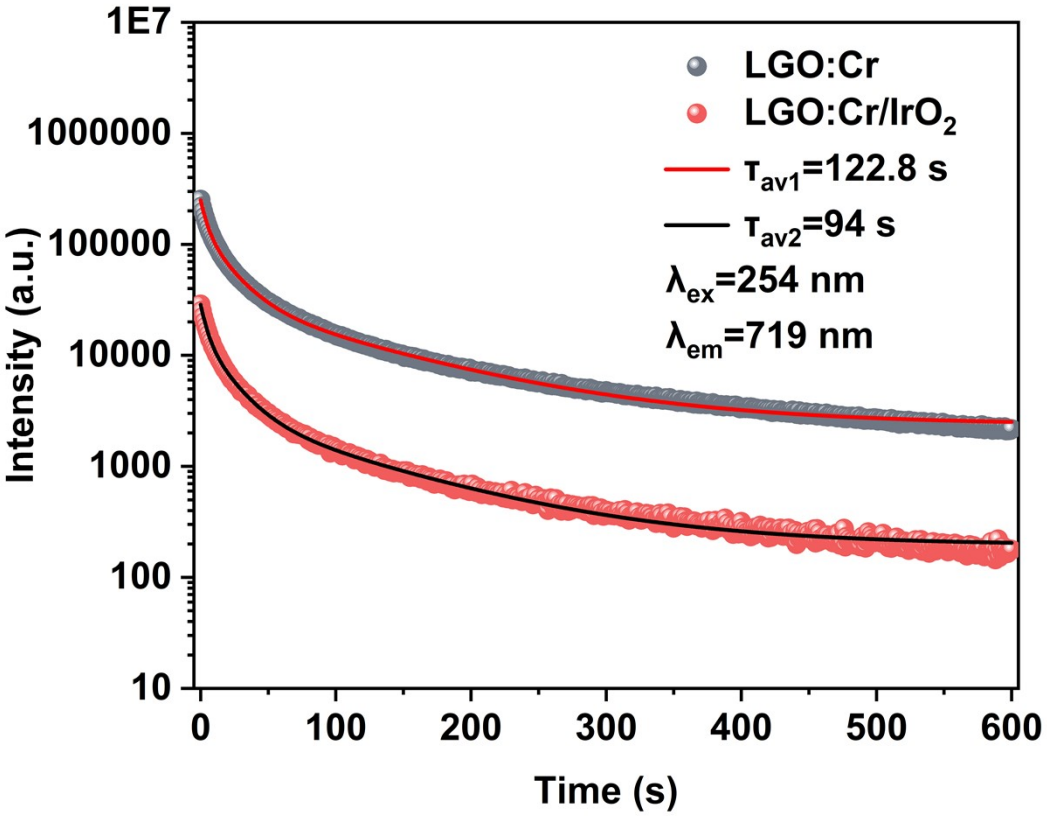

Figure S17. Afterglow decay curves of LGO:Cr and LGO:Cr/IrO_2 after 5 min of 254 nm UV light irradiation.

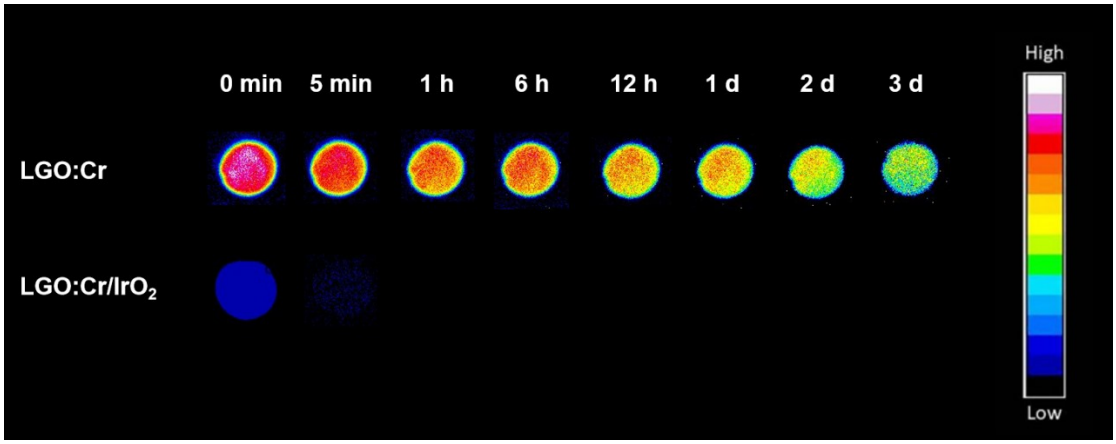

Figure S18. The afterglow decay images of samples were recorded by a charge-coupled device (CCD) camera with different interval times after 10 min of 254 nm UV irradiation.

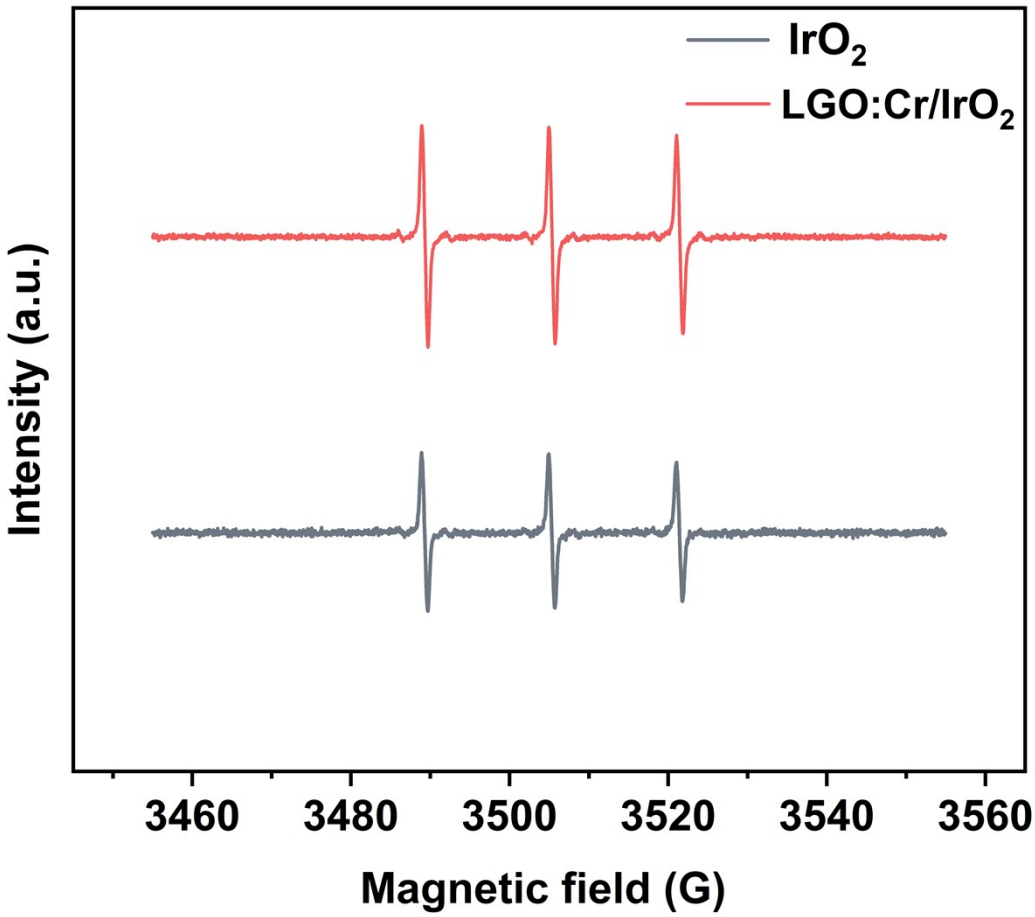

Figure S19. The ESR spectra of IrO_2 and LGO:Cr/IrO_2.

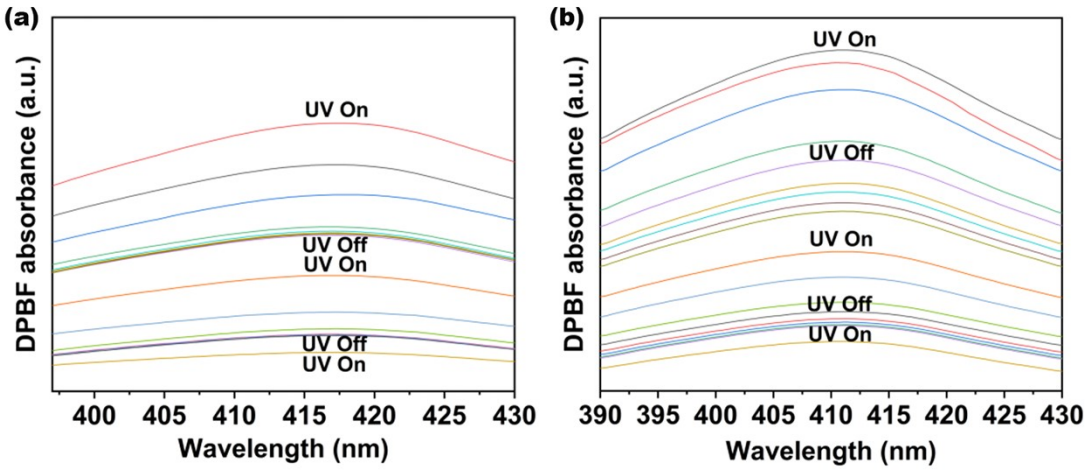

Figure S20. (a) UV-Vis absorbance spectra of DPBF in the DPBF and IrO_2 NPs mixed solution after being excited with UV lamp. (Absorbance was tested at two-minute intervals). (b) UV-Vis absorbance spectra of DPBF in the DPBF and LGO:Cr/IrO_2 mixed solution after being excited with UV lamp. (Absorbance was tested at two-minute intervals).

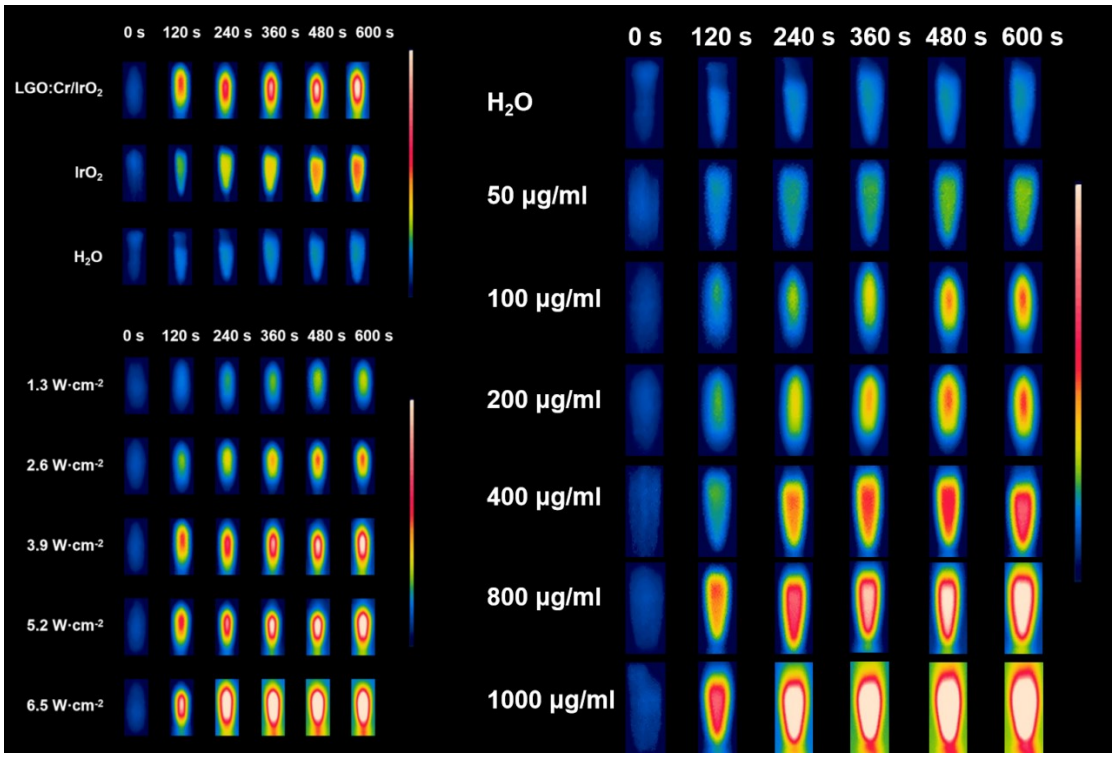

Figure S21. Photo-thermal photos taken by infrared thermal imager under different conditions.

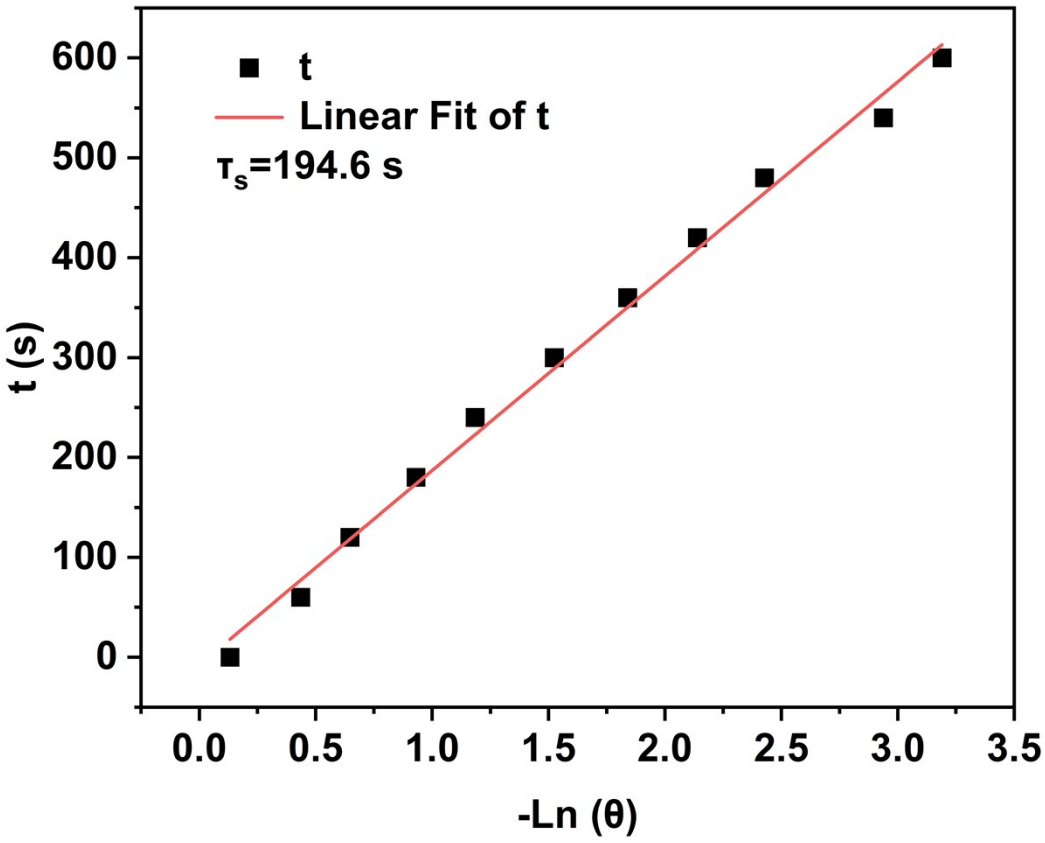

Figure S22. t vs -Ln (θ) fitting curve.